

DOI: 10.13526/j. issn. 1006-6144. 2019. 06. 018

## Ultrastrong Raman Enhancement on Gold Nanoparticle-Decorated Transition Metal Dichalcogenides Nanosheets for Molecule Detection

Jason D Orlando<sup>1</sup>, Ethan Kahn<sup>2</sup>, Cindy Y Wong<sup>3</sup>, Yin-ting Yeh<sup>4,5</sup>, Tej B Limbu<sup>1</sup>,  
Basant Chitara<sup>1</sup>, Ana L Elias<sup>4,5</sup>, Mauricio Terrones<sup>4,5</sup>, YAN Fei<sup>\*1</sup>

(1. Department of Chemistry and Biochemistry, North Carolina Central University, Durham, NC 27707, USA;

2. Department of Materials Science and Engineering, The Pennsylvania State University,  
University Park, PA 16802, USA;

3. School for Engineering of Matter, Transport and Energy, Arizona State University, Tempe, AZ 85287, USA;

4. Department of Physics, The Pennsylvania State University, University Park, PA 16802, USA;

5. Center for Nanoscale Science, The Pennsylvania State University, University Park, PA 16802, USA)

**Abstract:** A facile approach was developed for the decoration of monolayer tungsten disulfide(WS<sub>2</sub>) and molybdenum disulfide(MoS<sub>2</sub>) nanosheets with uniform gold nanoparticles with precisely controlled sizes, and their plasmonic properties were examined at different laser excitation wavelengths for trace detection of Rhodamine 6G(R6G) using surface-enhanced Raman scattering(SERS). Homogeneous deposition of gold nanoparticles on WS<sub>2</sub> and MoS<sub>2</sub> nanosheets was achieved by the reduction of hydrogen tetrachloroaurate via a seed-mediated growth method. The as-prepared heterostructures were characterized using scanning electron microscopy and Raman spectroscopy. Several substrates exhibited a Raman enhancement factor on the order of  $\sim 10^8$ , which is almost sufficient for the detection of single molecule. Our results demonstrate that controlled decoration of noble metal nanoparticles is a feasible and general strategy for structural modification of ultrathin transition metal dichalcogenides to develop highly-efficient and flexible substrates for next generation of SERS-based chemical and biological sensors.

**Keywords:** Transition metal dichalcogenides; Surface-enhanced Raman scattering; Rhodamine 6G; Gold nanoparticles

**CLC number:** O657.37

**Document code:** A

**Artical IC:** 1006-6144(2019)06-811-06

### Introduction

The ability to detect trace amounts of target analytes such as environmental pollutants, explosive hazards, and specific disease biomarkers has garnered enormous attention among the scientific community<sup>[1-3]</sup>. Surface-enhanced Raman scattering(SERS) is a potential technique to achieve minuscule level detection with specificity for choice analytes, it has been utilized for reproducible analyte detection of single-molecule quantities<sup>[4-5]</sup>. SERS was first discovered over 40 years ago when it was shown to enhance an analyte's Raman signal on a roughed silver electrode<sup>[6]</sup>. Since then, two contributing mechanisms for SERS have been developed, electromagnetic enhancement and chemical enhancement<sup>[7-8]</sup>. This work is aimed to build upon the efforts to develop novel SERS substrates. Using the well-known electromagnetic enhancement of gold on flexible opto-electronic transition

---

**Received date:** 2019-10-10

**Foundation item:** This study was supported in part by the U. S. National Science Foundation(Awards # 1831133 and # 1523617)

**\* Corresponding author:** Mr. Fei Yan, Ph. D. , Research interests: Analytical chemistry & materials chemistry.

E-mail: fyan@nccu.edu

metal dichalcogenides (TMDs) to create flexible substrates for SERS applications and study how varying parameters affect the enhancement seen from these hybrid materials<sup>[9-11]</sup>.

Two-dimensional(2D) layered materials have become an increasingly promising potential building block for chemical sensing. TMDs, and other 2D layered materials owe this potentiality to their tunable and intriguing electrical and optical properties<sup>[12]</sup>. As a result, 2D materials can exhibit plasmonic properties which is one application to pursue SERS-based sensing technology. 2D materials such as TMDs and graphene owe their SERS properties mainly to the chemical enhancement theory. By which the 2D material acts as charge donors and the analyte acceptors to increase the observed Raman signal from the analyte<sup>[13-15]</sup>. A large area of research on TMDs materials is focused on the future prospect of optimizing these atomically thin layered materials for transistors, semiconductors, and other opto-electronic devices. Due to their size and thickness this will allow for these devices to be nano scale, flexible, stretchable and transparent<sup>[10,11,16]</sup>. The fact that TMDs nanosheets can display SERS characteristics makes them an optimal choice for decorating with SERS active noble metal nanoparticles, beyond just providing a flexible substrate.

Gold nanoparticles(AuNPs) have been studied extensively for SERS since its discovery. AuNPs have been shown to provide remarkable Raman enhancement of up to  $10^{14}$ <sup>[17]</sup>. Gold has been employed for SERS through a variety of means. It has been utilized as a nanoscale gold tip above the substrate, AuNPs, AuNP coated in other metals or nonmetallic materials, surface-decorated substrates, and thin films<sup>[2,18-20]</sup>. The strong Raman enhancement observed combined with the versatility and ease of synthesis makes gold moieties an attractive SERS substrate or substrate component.

This work aims to open the door to the creation of reusable flexible SERS substrates consisting of AuNP-decorated TMDs heterostructures. Herein we report the SERS effectiveness of these substrates and their comparative efficacy under varying conditions such as nanoparticle size, laser frequency, and TMDs substrate used. AuNPs were created of various sizes with a seed mediated growth for comparison. Decoration was achieved through spin coating AuNP solutions onto as-grown TMDs substrates. The SERS effectiveness was measured through the detection of a model dye Rhodamine 6G(R6G).

## 1 Experimental

### 1.1 Apparatus and Materials

A Horiba LabRam HR Evolution was used to determine the number of layers for as grown TMDs along with carry out the SERS study after AuNPs decoration. A Fei Nova NanoSEM 630 was used to further characterize TMDs, observe AuNP size and decoration of the TMDs substrates.

Sulfur powder 99. 5% and  $\text{WO}_3$  powder 99. 999% were purchased from Alfa Aesar, 99% R6G was purchased from Acros Organic. NaBr 99%,  $\text{MoO}_2$  99%, Gold (III) chloride trihydrate > 99. 9%, Hexadecyltrimethylammonium bromide(CTAB) >99%, 2.5%  $\text{AgNO}_3$  solution, 99% L-ascorbic acid, >99. 0% sodium citrate tribasic dehydrate, and 98% sodium borohydride were purchased from Sigma Aldrich. All aqueous solutions were prepared by deionized(DI) water unless specified otherwise.

### 1.2 Growth of $\text{MoS}_2$ and $\text{WS}_2$ Nanosheets

$\text{MoS}_2$  and  $\text{WS}_2$  samples were grown in a Thermo Scientific Lingberg Blue M chemical vapor deposition (CVD) furnace.  $\text{MoS}_2$  growth was done on  $\text{SiO}_2/\text{Si}$  wafers. The wafers were placed polished side down over the sample boat in the center of the tube furnace. The sample boat contained 1 mg of a 10:1 mixture of  $\text{MoO}_2$  and NaBr by weight. 100 mg of sulfur powder was placed in a sample boat just outside the tube furnace with this portion of the tube covered with a heating rope. The Furnace was heated to 800 °C over the course of 20 min and held at this temperature for 5 min. Sulfur was heated to 220 °C and carried downstream by 100 standard cubic centimeters per minute(sccm) of Ar. After 5 min, the furnace is cracked open to increase the cooling rate. The  $\text{WS}_2$  growth followed a similar procedure. The inner furnace sample boat held 10:1 ratio of  $\text{WO}_3$  and NaBr for the tungsten precursor. The furnace was ramped to 825 °C over the course of 20 min and held for 10 min. The

heating rope was set to heat the sulfur at 220 °C and carried through the tube by a flow of 200 sccm Ar.

### 1.3 Growth of Gold Nanoparticles

AuNPs were grown via a seed mediated growth. The seed solution was created by first placing a 0.1 mol/L solution of NaBH<sub>4</sub> on ice. A 25 mL reaction vial was filled with 18 mL of DI water to which 50  $\mu$ L of 0.1 mol/L HAuCl<sub>4</sub>, 50  $\mu$ L of 0.1 mol/L sodium citrate, 600  $\mu$ L of the chilled NaBH<sub>4</sub>, and sonicated until thoroughly mixed. The growth solution to which the seed solution would be added was made with 10 mL 0.1 mol/L CTAB, 350  $\mu$ L 0.1 mol/L L-ascorbic acid, 250  $\mu$ L 0.1 mol/L HAuCl<sub>4</sub>, and 50  $\mu$ L 0.1 mol/L AgNO<sub>3</sub>. Three separate solutions of this growth solution were created to which different quantities of seed solution were added. 25, 5, 0.5  $\mu$ L were added to one of the three solutions with DI water so the total amount of added liquid to the solution was 25  $\mu$ L. Each solution was centrifuged at 4 750 r/min for 1 h. the precipitate was resuspended in DI water and the process was repeated several times to wash the grown particles.

## 2 Results and Discussion

### 2.1 Synthesis and Characterization of MoS<sub>2</sub> and WS<sub>2</sub> Nanosheets

MoS<sub>2</sub> and WS<sub>2</sub> nanosheets were grown according to the aforementioned procedure to optimize the growth of monolayer island samples. TMDs such as MoS<sub>2</sub> and WS<sub>2</sub> have indirect band gaps in their bulk form. As monolayers these structures have sizable direct band gaps. This gives them interesting optoelectronic properties for sensing and potential nanoelectronics, making them the ideal form for the heterostructure SERS substrates<sup>[21]</sup>. Fig. 1 shows the E<sub>2g</sub><sup>1</sup> and A<sub>1g</sub> stretching modes of the grown MoS<sub>2</sub> and WS<sub>2</sub> nanosheets. Monolayer WS<sub>2</sub> has these stretching modes in at 356 and 417.5  $\text{cm}^{-1}$ , which is good agreement with our experiment results<sup>[22]</sup>. Like with WS<sub>2</sub> observing the change in the difference between these two stretching modes for MoS<sub>2</sub> gives insight into the number of layers in the sample. Sub 20  $\text{cm}^{-1}$  difference between these modes is an indicator of monolayered material, which is observed in the grown sample<sup>[23]</sup>. The Raman data indicates the substrates used were monolayer MoS<sub>2</sub> and WS<sub>2</sub>, respectively.

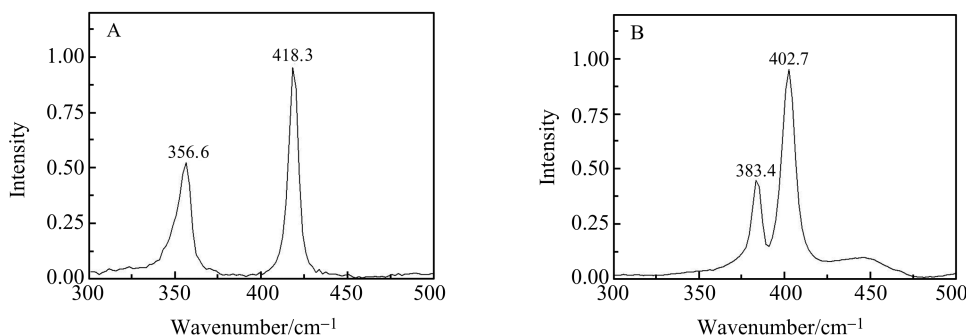


Fig. 1 Raman spectra with a 488 nm laser excitation of as-grown TMDs to confirm monolayer growth

(A) WS<sub>2</sub> was observed to have Raman shifts at 356.57 and 418.28  $\text{cm}^{-1}$ ; (B) MoS<sub>2</sub> was observed to have Raman shifts at 383.43 and 402.69  $\text{cm}^{-1}$ .

图1 用488 nm激光激发下的拉曼光谱来确认单层生长

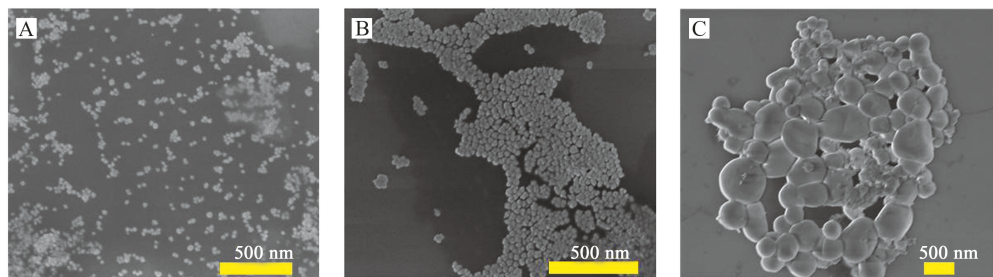
(A) WS<sub>2</sub> 在 356.57 和 418.28  $\text{cm}^{-1}$  处有拉曼位移; (B) MoS<sub>2</sub> 在 383.43 和 402.69  $\text{cm}^{-1}$  处有拉曼位移。

### 2.2 Synthesis and Characterization of AuNPs

AuNPs were synthesized via two different methods discussed above. The AuNPs solutions were then spin coated onto the SiO<sub>2</sub>/Si wafers that the TMDs were grown on for SERS applications. Fig. 2 shows a standardized size comparison between the particles and their coverage. After drying the applied AuNPs solution onto the TMDs substrates  $1.0 \times 10^{-6}$  mol/L R6G solution was spin coated onto the surface for SERS. These as prepared substrates were analyzed under two different laser frequencies to compare size of AuNPs, type of substrate, and frequency dependence.

### 2.3 SERS Characteristics of AuNPs-Decorated MoS<sub>2</sub> and WS<sub>2</sub> Nanosheets

Fig. 3 shows the spectra that were obtained when probing SERS effectiveness of the created substrates at

Fig. 2 SEM images of as-grown AuNPs on  $\text{MoS}_2$  and  $\text{WS}_2$  nanosheets

(A) 25 nm, (B) 35 nm, and (C) 400 nm prior to SERS study or addition of R6G. Scale bar: 500 nm.

图2 长在  $\text{MoS}_2$  和  $\text{WS}_2$  纳米片上的 AuNP<sub>3</sub> 的扫描电子显微镜(SEM)图像

(A) 25 nm; (B) 35 nm; (C) 400 nm.

different laser frequencies for the spectra of R6G obtained at 5% laser power<sup>[24]</sup>. Immediately upon observation a size contingency is observed across the samples which is to be expected based on previous SERS studies of AuNPs size<sup>[25]</sup>. The largest AuNPs exhibited little to no SERS on the detection of the choice analyte, and the 25 nm sized AuNPs containing substrates had the best enhancement. The 35 nm AuNPs substrates produced enhancement to a lesser degree than the 25 nm samples in every sample that enhancement could be observed. 10 nm sized AuNPs proved difficult to acquire spectra with any enhancement at all except for on the  $\text{WS}_2$  substrate under the 488 nm laser excitation.

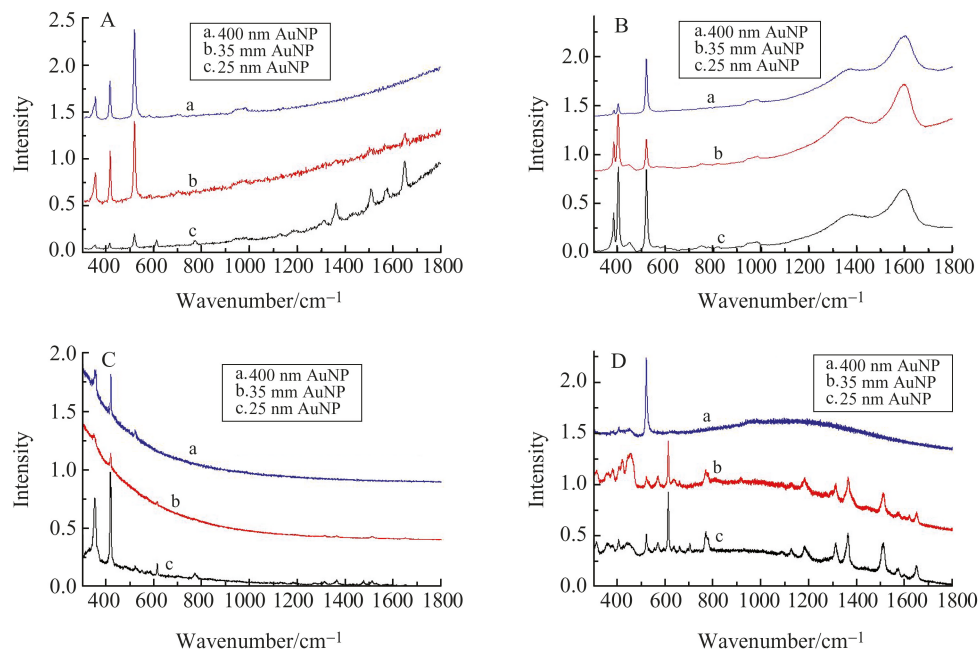
Fig. 3 Surface-enhanced Raman spectra of  $1.0 \times 10^{-6}$  mol/L R6G on AuNP decorated TMDs substrates.  $\text{WS}_2$  under 488 nm (A),  $\text{MoS}_2$  under 488 (B),  $\text{WS}_2$  under 633 nm (C), and  $\text{MoS}_2$  under 633 nm (D)

图3 表面增强拉曼光谱

$1.0 \times 10^{-6}$  mol/L R6G 的在金颗粒修饰的  $\text{WS}_2$  上, 488 nm 激光激发 (A); 在金颗粒修饰的  $\text{MoS}_2$ , 488 nm 激光激发 (B); 金颗粒修饰的  $\text{WS}_2$  上, 633 nm 激光激发 (C); 金颗粒修饰的  $\text{MoS}_2$  上, 633 nm 激光激发 (D)

The spectra of the  $\text{MoS}_2$  substrate under the 488 nm laser excitation were dominated by fluorescence of the R6G. As a result, R6G peaks were unable to be resolved from this. This was seen across all the spectra obtained for this substrate under these parameters and is surprising since AuNPs have fluorescence quenching properties and the fluorescence was not seen on any of the other test conditions to this level<sup>[26]</sup>. Potentially indicating a parameter of the substrate or test is at play.

The best performing substrate for SERS for the two TMD substrates was not under the same laser frequency, though it was with the same size AuNPs. The use of the 488 nm laser produced the strongest

enhancement with  $\text{WS}_2$  across all substrate conditions that exhibited any enhancement. While with  $\text{MoS}_2$  the strongest enhancement came under the 633 nm laser excitation, as fluorescence dominated the spectrum under the 488 nm laser excitation. Upon 633 nm laser excitation,  $\text{MoS}_2$  nanosheets decorated with 25 nm and 35 nm AuNPs exhibited an analytical enhancement factor(AEF) on the order of  $10^7\text{--}10^8$ , which is comparable to other SERS substrates and sufficient for the detection of single molecule. AEF was calculated by  $\text{AEF} = \frac{I_{\text{SERS}}/C_{\text{SERS}}}{I_{\text{RS}}/C_{\text{RS}}}$ , where  $I_{\text{SERS}}$  and  $C_{\text{SERS}}$  are the intensity and concentration of the dye on the SERS samples and  $I_{\text{RS}}$  and  $C_{\text{RS}}$  are the intensity and concentration on samples containing only dye<sup>[1,27]</sup>. This may point to some specificity in the laser frequency choice which could be selected to detect certain analytes over others utilizing the differing substrates.

### 3 Conclusion

AuNPs-decorated  $\text{MoS}_2$  and  $\text{WS}_2$  nanosheets were synthesized for potential use as flexible SERS substrates. Their SERS properties were studied at different laser excitation wavelengths. It was discovered that the degree of Raman enhancement is contingent on the size of AuNPs. Additionally, the different substrates used performed best under different laser frequencies, allowing for some potential specificity in detection based on fabrication. Among all the substrates tested,  $\text{MoS}_2$  nanosheets decorated with 25 nm and 35 nm AuNPs exhibited the best AEF( $\sim 10^7\text{--}10^8$ ) under the 633 nm excitation for the detection of R6G. This work points to some potential application for decorated TMDs as novel substrates for SERS-based sensing. Looking into the specificity of these fabricated substrates and shape related contingencies of the AuNPs used, reliable flexible 2D sensors could be utilized to detect trace amounts of specific analytes.

### References:

- [1] Ben-Jaber S, Peveler W J, Quesada-Cabrera R, Cortés E, Sotelo-Vazquez C, Abdul-Karim N, Maier S A, Parkina I P. *Nature Communications*, 2016, **7**:12189.
- [2] Halvorson R A, Vikesland P J. *Environmental Science & Technology*, 2010, **44**(20):7749.
- [3] Yilmaz M, Babur E, Ozdemir M, Giesecking R L, Dede Y, Tamer U, Schatz G C, Facchetti A, Usta H, Demirel G. *Nature Materials*, 2017, **16**:918.
- [4] Tanwar S, Haldar K, Sen T J. *Journal of the American Chemical Society*, 2017, **139**:17639.
- [5] Ru E C L, Meyer M, Etchegoin P G. *Journal of Physical Chemistry B*, 2006, **110**(4):1944.
- [6] Fleischmann M, Hendra P J, McQuillan A J. *Chemical Physics Letters*, 1974, **26**(2):163.
- [7] Jeanmaire D L, Duyne R P V. *Journal of Electroanalytical Chemistry and Interfacial Electrochemistry*, 1977, **84**(1):1.
- [8] Albrecht M G, Creighton J A. *Journal of the American Chemical Society*, 1977, **9**(15):5215.
- [9] Gao P, Patterson M L, Tadayyon M A, Weaver M J. *Langmuir*, 1985, **1**(1):173.
- [10] Akinwande D, Petrone N, Hone J. *Nature Communications* 2014, **5**:5678.
- [11] Gao L. *Small*, 2017, **13**(35):1603994.
- [12] Anichini C, Czepa W, Pakulski D, et al. *Chemical Society Reviews*, 2018, **47**:4860.
- [13] Stiles P L, Dieringer J A, Shah N C, Duyne R P V. *Annual Review of Analytical Chemistry*, 2008, **1**(1):601.
- [14] Lee Y, Kim H, Lee J, Yu S H, Hwang E, Lee C, Ahn J, Cho J H. *Chemistry of Materials*, 2015, **28**(1):180.
- [15] Song X, Wang Y, Zhao F, et al. *ACS Nano*, 2019, **13**(7):8312.
- [16] Jariwala D, Sangwan V K, Lauhon L J, Marks T J, Hersam M C. *ACS Nano*, 2014, **8**(2):1102.
- [17] Tian Z Q, Ren B, Li J F, Yang Z L. *Chemical Communications*, 2007, 3514.
- [18] Li J F, Huang Y F, Ding Y, et al. *Nature*, 2010, **464**(7287):392.
- [19] Park S, Yang P, Corredor P, Weaver M J. *Journal of the American Chemical Society*, 2002, **124**(11):2428.
- [20] Ngo Y H, Then W L, Garnier G. In *Advances in Pulp and Paper Research*, Cambridge 2013, *Trans. of the XVth Fund. Res. Symp.* Cambridge, 2013, (S. J. I'Anson, ed.), FRC, Manchester, 2018:967.
- [21] Wang Q H, Kalantar-Zadeh K, Kis A, Coleman J N, Strano M S. *Nature Nanotechnology*, 2012, **7**(11):699.
- [22] Berkdemir A, Gutiérrez H R, Botello-Méndez A R, et al. *Scientific Reports*, 2013, **3**(1):1755.

- [23] Lee C, Yan H, Brus L E, Heinz T F, Hone J, Ryu S. ACS Nano, 2010, **4**(5), 2695.
- [24] Jensen L, Schatz G C. The Journal of Physical Chemistry A, 2006, **110**(18), 5973.
- [25] Hong S, Li X. Journal of Nanomaterials, 2013, 790323.
- [26] Schneider G, Decher G, Nerambourg N, Praho R, Werts M H V, Blanchard-Desce M. Nano Letters, 2006, **6**(3), 530.
- [27] Le Ru E C, Meyer B M, Etchegoin P G. Journal of Physical Chemistry C, 2007, **111**, 13794.

## 基于超强拉曼增强金纳米粒子修饰的过渡金属双硫属化合物纳米片的分子检测

Jason D Orlando<sup>1</sup>, Ethan Kahn<sup>2</sup>, Cindy Y Wong<sup>3</sup>, Yin-ting Yeh<sup>4,5</sup>, Tej B Limbu<sup>1</sup>, Basant Chitara<sup>1</sup>, Ana L Elias<sup>4,5</sup>, Mauricio Terrones<sup>4,5</sup>, 鄭 非<sup>\*1</sup>

(1. Department of Chemistry and Biochemistry, North Carolina Central University, Durham, NC 27707, USA;

2. Department of Materials Science and Engineering, The Pennsylvania State University; University Park, PA 16802, USA;

3. School for Engineering of Matter, Transport and Energy, Arizona State University, Tempe, AZ 85287, USA;

4. Department of Physics, The Pennsylvania State University; University Park, PA 16802, USA;

5. Center for Nanoscale Science, The Pennsylvania State University, University Park, PA 16802, USA)

**摘要:**本文报道用不同尺寸的金纳米粒子(AuNPs)来修饰单层 WS<sub>2</sub> 和 MoS<sub>2</sub> 纳米片,通过表面增强拉曼散射(SERS)技术检测微量的罗丹明 6G 染料,并对比了它们在不同波长的激光激发下的等离子体特性。AuNPs 在 WS<sub>2</sub> 和 MoS<sub>2</sub> 纳米片上的均匀沉积是通过种子介导的生长方法还原 HAuCl<sub>4</sub> 来实现的。我们进一步使用扫描电子显微镜和拉曼光谱对所制备的异质结构进行了表征。几种优化结构的拉曼增强因子接近 10<sup>8</sup>,几乎达到检测单分子需要的灵敏度。我们的研究结果表明,通过贵金属纳米粒子对超薄过渡金属双硫属元素化合物进行可控修饰是完全可行的。这个策略也适合于制备高效且灵活的基底,用在新一代基于表面增强拉曼散射的化学传感器和生物传感器上。

**关键词:**过渡金属双硫属元素化合物;表面增强拉曼散射;罗丹明 6G;金纳米颗粒